MB 11/11/96

LASER EMISSIVITY FREE THERMOMETRY APPLIED TO A LEVITATED DROP.

Author: Russell Goyder.
Project Supervisor: Dr. G. J. Edwards.

Centre for Quantum Metrology, National Physical Laboratory, Teddington, Middlesex, TW11 0LW.

Except where specific reference is made to the work of others, this work is original and has not been already submitted either wholly or in part to satisfy and degree requirement at this or any other university.

Signed: 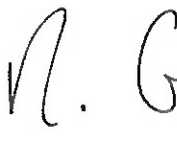 (R. Goyder.)

SUMMARY

Radiation thermometry is a well established technique and is used to define the International Temperature Scale (ITS90) for temperatures above 962°C, but is limited as a general method of temperature measurement by the need to know the emissivity function of the radiating body. Laser Absorption Radiation Thermometry (LART), of which Laser Emissivity Free Thermometry (LEFT) is a part, enables temperature to be measured without prior knowledge of emissivity, by using lasers to modulate the temperature of the body and detecting the radiation due to that modulation. Experimental trials of a LART system in a laboratory environment have yielded encouraging results. This prompted a further stage of development; an assessment of the technique as applied to a sample similar to that which may be encountered in a typical industrial environment; a levitated metal drop.

The levitated drop experiment in question was being carried out in the Centre for Materials Measurement and Technology (C.M.M.T.) within the National Physical Laboratory. It consisted of a copper coil (made of pipe so that water could flow inside as a coolant) in which flowed an AC current of about 300 kHz (radio frequencies). Inside this coil was a tube of square cross-section made of optical quartz, in which a metal drop, ~5mm in diameter, was levitated. It was also heated as a result of currents induced by the coil's changing magnetic field. So that the oxidation of the surface of the drop could be controlled, a variable mixture of Hydrogen and Argon gases flowed inside the tube. The coil was wound such that there was a gap separating its upper and lower portions, so that emitted radiation could be focused onto the detectors.

The LEFT system was tested using a high emissivity (inconel) sample in a furnace. As the uncertainty in any measurement was of primary interest the system was not calibrated and so no temperature measurement was made, however, the system was seen to perform as expected and so could be applied to the levitated drop. In the construction of the LEFT system, a major problem to be overcome was logistical, in that the whole system needed to be portable and compact. The optics were assembled on a 1.2×0.6m breadboard which was supported on a trolley with variable height and levelling adjustments, and the controlling electronics placed on a separate trolley. Additional difficulties were encountered when the RF field of the levitated drop experiment was found to interfere with a component of the thermometer, but the unwanted signal was removed by filtering.

With the levitated drop as a target, the signal to noise ratios of the two signals used by LEFT were found to be far too large to make a practical measurement. The phenomena giving rise to this large noise voltage were investigated and it was found that they could be overcome when the drop was in its solid phase, but with a liquid drop it was harder. Suggestions are made for further work to improve the signal to noise ratio and the project stimulated thought concerning modifying the LEFT system to render it insensitive to random fluctuations in sample emissivity.

Laser Emissivity Free Thermometry applied to a levitated drop.

Russell Goyder, 1st October 1996,

Centre for Quantum Metrology, National Physical Laboratory, Teddington, Middlesex, TW11 0LW.

ABSTRACT

Radiation thermometry is a well established technique and is used to define the International Temperature Scale (ITS90) for temperatures above 962°C, but is limited as a general method of temperature measurement by the need to know the emissivity function of the radiating body. Laser Absorption Radiation Thermometry (LART), of which Laser Emissivity Free Thermometry (LEFT) is a part, enables temperature to be measured without prior knowledge of emissivity, by using lasers to modulate the temperature of the body and detecting the radiation due to that modulation. Experimental trials of a LART system in a laboratory environment have yielded encouraging results. This has prompted a further stage of development, which is an assessment of the technique as applied to a sample similar to that which may be encountered in a typical industrial environment; a levitated metal drop. It was found that although temperature measurement was possible, the uncertainty was too large to make the measurement useful due to sources of noise associated with certain properties of the drop. Several ways in which this result may be improved are suggested.

PART 1: THE LASER EMISSIVITY FREE THERMOMETER

1.1 INTRODUCTION AND THEORY OF LEFT

Laser Absorption Radiation Thermometry[1] is a way of measuring temperature through the use of lasers. Laser radiation is modulated (chopped) at a certain frequency and so, when incident on a body, modulates the temperature of that body at the same frequency. This produces a fluctuation in the intensity of the radiation emitted by the body, the amplitude of which is measured using phase sensitive detection. Three separate techniques employing the above idea enable a temperature measurement to be made. One of these is called Laser Emissivity Free Thermometry (LEFT) and involves two lasers chopped at two different frequencies. The ratio of the amplitudes of the signals due to these lasers can give a temperature measurement that is independent of emissivity with an important condition; if one of the lasers emits radiation at a certain wavelength, say λ_1, and the signal due to that laser is detected at some other wavelength, say λ_2, then the second laser in the system must emit radiation at wavelength λ_2 and the signal due to that laser must be detected at wavelength λ_1. The following arguments formally show that this is true.

Figure 1. Laser beam incident on sample

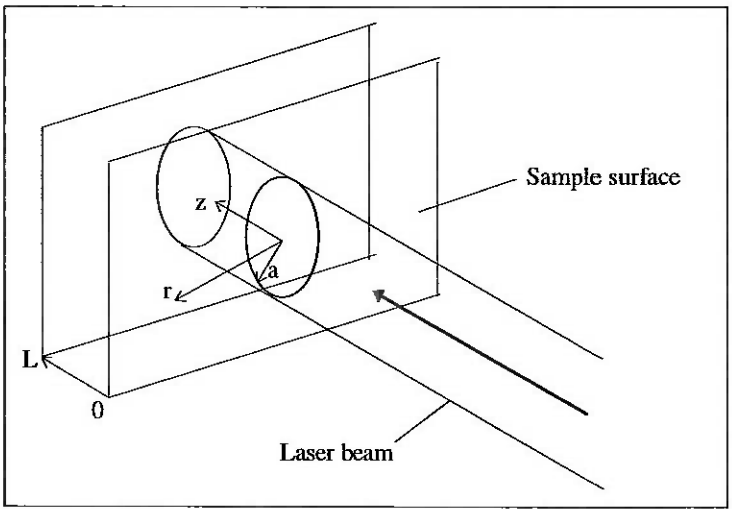

Consider the effect of a laser beam incident on a surface, as shown in figure 1.

A mathematical model of the heat flow in the target region of the sample, yields an inhomogeneous diffusion equation:

$$\nabla^2 T - \frac{1}{D}\frac{\partial T}{\partial t} = \frac{-G(r,t)}{K} \qquad (1)$$

where: D = thermal diffusivity = K/C_v,
G(r,t) = heat input per unit volume,
K = thermal conductivity,
C_v = heat capacity at constant volume.

The symmetry of the system makes it most convenient to use cylindrical polar co-ordinates.
If the laser beam's intensity has a Gaussian radial dependence, the heat input can be expressed as:

$$G(r,t) = \frac{\varepsilon\beta}{\pi r^2} P_w e^{-2r^2/a^2} e^{-\beta z} e^{j\omega t} + c.c. \tag{2}$$

where: P_ω = beam power at frequency ω,
ε = surface emissivity,
β = sample absorption coefficient,
a = Gaussian radius of laser beam,
c.c. = complex conjugate.

For G = 0 (the homogeneous problem), the solution of equation (1) is:

$$T_1(r,z,t) = Be^{j\omega t} \int_0^\infty \frac{ue^{-u^2a^2/8}}{\eta^2 - u^2} J_0(ur)[c(u)e^{-\alpha z} + d(u)e^{\alpha z}]du + c.c. \tag{3}$$

where: $B = \frac{\varepsilon\beta P_\omega}{4\pi K}$ $\alpha^2 = u^2 + \frac{j\omega}{D}$ $\eta^2 = \beta^2 - \frac{j\omega}{D}$

J_0 is a Bessel function of order 0.and c(u) and d(u) are two arbitrary constants, to be determined by the boundary conditions of the problem.

With the above form of the heat input function, the particular integral of equation (1) can be written:

$$T_2(r,z,t) = Be^{\beta z} e^{j\omega t} \int_0^\infty \frac{ue^{-a^2u^2/8}}{\eta^2 - u^2} J_0(ur)du + c.c. \tag{4}$$

and thus, the general solution is obtained from the sum of equations (3) and (4).

If it is assumed that heat is lost linearly at the sample surface, i.e.

$$\frac{\partial T}{\partial z} = \mu T \quad (z = 0), \qquad \frac{\partial T}{\partial z} = -\mu T \quad (z = L) \quad (\mu > 0)$$

then the arbitrary constants c and d can be obtained from:

$$-c(\alpha + \mu) + d(\alpha - \mu) = \beta + \mu \tag{5}$$

and

$$-c(\alpha - \mu)e^{-\alpha L} + d(\alpha + \mu)e^{\alpha L} = (\beta - \mu)e^{-\beta L} \tag{6}$$

Considering the situation at the surface and making the approximation $\beta L \gg 1$ (i.e. a thick sample) changes the general solution to:

$$T(r,0,t) = Be^{j\omega t} \int_0^\infty \frac{ue^{-u^2a^2/8}}{(\eta^2 - u^2)} J_0(ur)[1 + c(u) + d(u)]\, du + c.c. \tag{7}$$

The pair of simultaneous equations, (5) and (6), gives c(u) and d(u) to be

$$c(u) = \frac{\beta(\alpha+\mu)e^{2\alpha L}}{X} \qquad d(u) = \frac{\beta(\alpha-\mu)}{X}$$

where: $$X = (\alpha-\mu)^2 - (\alpha+\mu)^2 e^{2\alpha L}$$

and so the general solution can be written as:

$$T(r,0,t) = \frac{\varepsilon P_\omega}{4\pi K}\int_0^\infty u e^{-u^2a^2/8} g(u) J_0(ur) e^{j\omega t}\, du + c.c. \tag{8}$$

where:

$$g(u) = \frac{C+D}{\beta} = \frac{\alpha-\mu+(\alpha+\mu)e^{2\alpha L}}{(\alpha-\mu)^2-(\alpha+\mu)^2 e^{2\alpha L}}$$

For a small temperature rise, the power radiated from the target area is:

$$Q(\lambda,T) = \varepsilon L'(\lambda,T_0)\Omega\Delta\lambda\int_S T dS \tag{9}$$

where:
- Ω = detection solid angle,
- $\Delta\lambda$ = optical bandwidth,
- ε = emissivity,
- T_0 = ambient temperature.
- L' = the first derivative of the Planck black body radiance function with respect to temperature,
- S = Area of view of detector.

So by substituting the temperature rise, T into the above equation, the radiated power becomes:

$$Q(\lambda,T) = \varepsilon L'(\lambda,T)\Omega\Delta\lambda\int_S \left(\frac{\varepsilon P_\omega}{4\pi K}\int_0^\infty u e^{-u^2a^2/8} g(u) J_0(ur) e^{j\omega t}\, du + c.c.\right) dS \tag{10}$$

$$\therefore \quad Q(\lambda,T) = \varepsilon_2 L'(\lambda,T)\Omega\Delta\lambda\frac{\varepsilon_1 P_\omega}{4\pi K}\int_S\int_0^\infty \left(u e^{-u^2a^2/8} g(u) J_0(ur) e^{j\omega t} du + c.c.\right) 2\pi r dr \tag{11}$$

$$\therefore \quad Q(\lambda,T) = A\int_0^\infty\int_0^\infty u J_0(ur) dr\, e^{-u^2a^2/8} g(u)\, du + c.c.$$

where: $$A = \frac{\varepsilon_1\varepsilon_2 L'(\lambda_2,T)\Omega\Delta\lambda P_\omega e^{j\omega t}}{2K}$$

and where:
- ε_1 = emissivity at laser beam wavelength λ_1
- ε_2 = emissivity at radiated wavelength, λ_2.

The area of integration over the sample surface can be approximated to infinity if the active area of the photodiodes is greater than the area over which the heat from the laser beam has time to flow.

$$\therefore \quad Q(\lambda,T) = A\int_0^\infty \delta(u) g(u) e^{-u^2a^2/8} du$$

$$\therefore \quad Q(\lambda_2, T) = \frac{\varepsilon_1 \varepsilon_2 L'(\lambda_2, T) \Omega \Delta\lambda P_\omega e^{j\omega t}}{2K} g(0)$$

As can be seen above, the product of the emissivities $\varepsilon_1\varepsilon_2$ appears in the expression for radiated power, and therefore also in the expression for the detector current due to this radiation, below:

$$I_2 = R_2 C_2 Q(\lambda_2, T) \tag{12}$$

where: R_2 = detector responsivity at wavelength λ_2,
C_2 = transmission factor through optics at wavelength λ_2.

The detector current at wavelength λ_1 due to the radiation produced by a laser at wavelength λ_2 can be written by interchanging the suffices of equation (12):

$$I_1 = R_1 C_1 Q(\lambda_1, T) \tag{13}$$

The ratio of the above two currents yields the temperature of the body as the product $\varepsilon_1 \varepsilon_2$ cancels and all other terms are either measurable or known. In practice they are collected together and form a calibration constant.

1.2 THERMAL IMAGING AND DETECTION

Experimental Method[2]

The thermal imaging apparatus was assembled along a rail attached to a 120 × 60 cm optical breadboard as shown in figure 2. It consisted of three pairs of plano-convex doublets (chosen to minimise spherical aberration) that focused radiation from the sample hot body onto the two detectors. Interference filters were placed in front of the two detectors, chosen to have maximum transmitance at the two wavelengths of the light emitted by the lasers, namely 840nm and 1320nm. A beam splitter placed at 45° to the optic axis inside the detector cube was used to separate the beam. Its maximum transmitance was at 840nm and maximum reflectance at 1320nm.

Figure 2. Thermal imaging apparatus

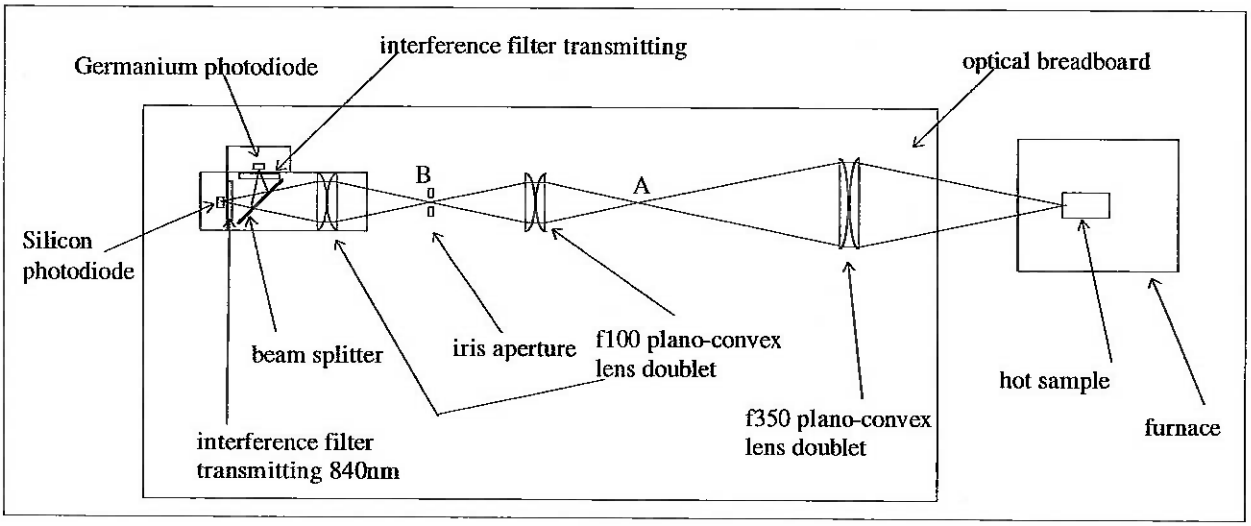

Positioning and alignment of the components was achieved by shining a visible (diode) laser spot onto a screen at the target position which acted as a point source then focusing its image at points A, B and at the detector positions. The alignment was checked by shining the laser onto a screen at point B and repeating the above except

voltage would have produced changes in temperature and hence radiance. The inconel sample's size (~500g) and the insulation in the furnace meant that it had a thermal time constant well in excess of that of the Lock-in amplifiers'.

To find out how well the beam was focused, the beam profile was measured, both as it emerged from the laser and at the target position. This was achieved by dragging a knife edge across the beam in front of a Germanium photodiode. The knife edge was mounted on a plate that could be moved using a micrometer barrel, and the curve obtained was differentiated to provide an approximate profile. It would only be a true profile if the beam intensity did not vary in the direction of movement of the knife edge or if a circular aperture was used, but in this there is the additional difficulty of finding the centre of the beam with sufficient accuracy. However, this method was sufficient for the purpose of giving a measure of the limits of the beam.

After this (sub)experiment, the Germanium detector was placed as shown so as to capture the beam reflected by the beam splitter at point C, in order to monitor the YAG laser power during the rest of the experiment.

As explained above, only two wavelengths of radiation are used by the system. This creates the problem of scattered laser radiation being detected and mistaken for induced thermal modulation, or even damaging the detectors. The scheme employed to overcome this problem is shown in figure 4. It uses two monostable multi vibrator chips, one to turn the lasers on a set time after it receives the down-going edge of the isolation chopper reference square wave and the other to turn the lasers off after another set time. Both these times could be adjusted and so any chopper frequency could be used. In practice, 300Hz was used and the system was set up by displaying the output of the channel 2 (Germanium) detector and the laser power supply voltage on an oscilloscope. Severe ringing in the detector was observed when the two times were not set correctly.

This 300Hz signal was then passed through an AND gate with the 16Hz TTL output the function generator that was the channel 1 Lock-in amplifier's reference signal, and then into the YAG laser itself.

To include the diode laser, the mirror at the top of the height change was replaced by a beam splitter allowing the passage of 840nm radiation but reflecting that of the YAG laser. It was aligned in the same way as the YAG laser and the laser back scatter elimination technique was set up as previously only using the Channel 1 (Silicon) detector. The path length of this beam was chosen to be identical to that of the YAG laser so it would be focused by the lens at point D. This is the reason, along with the need to protect the optical fibre, for having the mirror at point E.

Figure 4. Laser back-scatter elimination scheme

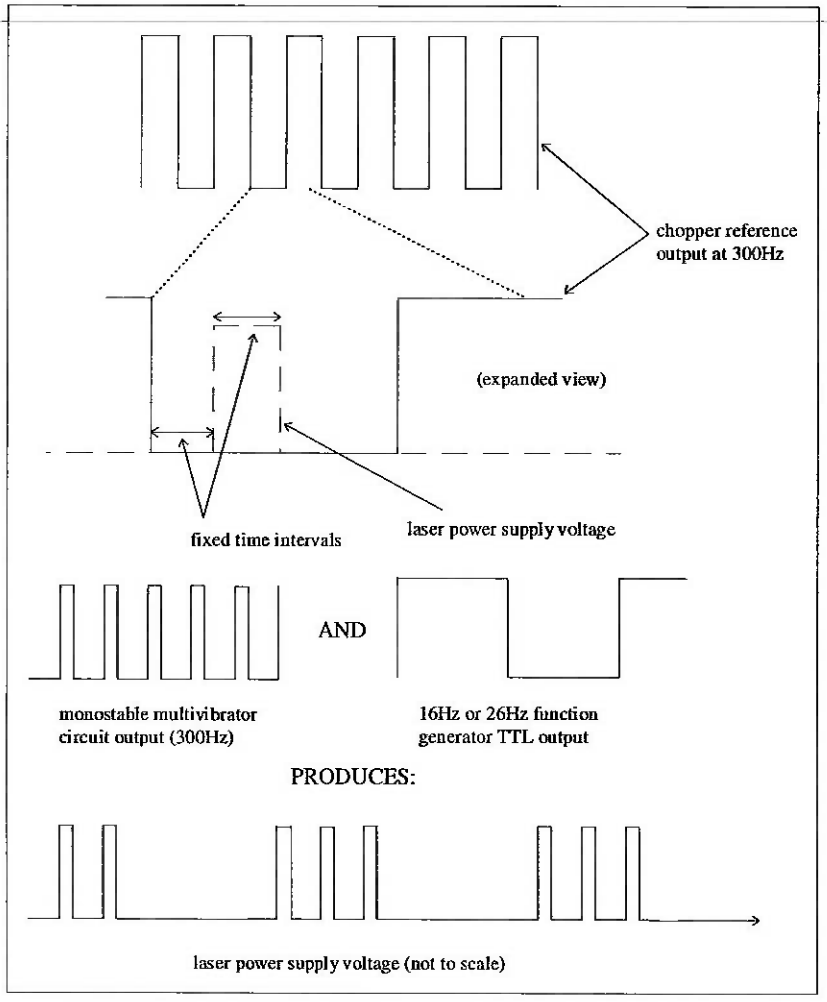

Figure 5. Introduction of the Diode laser into the system

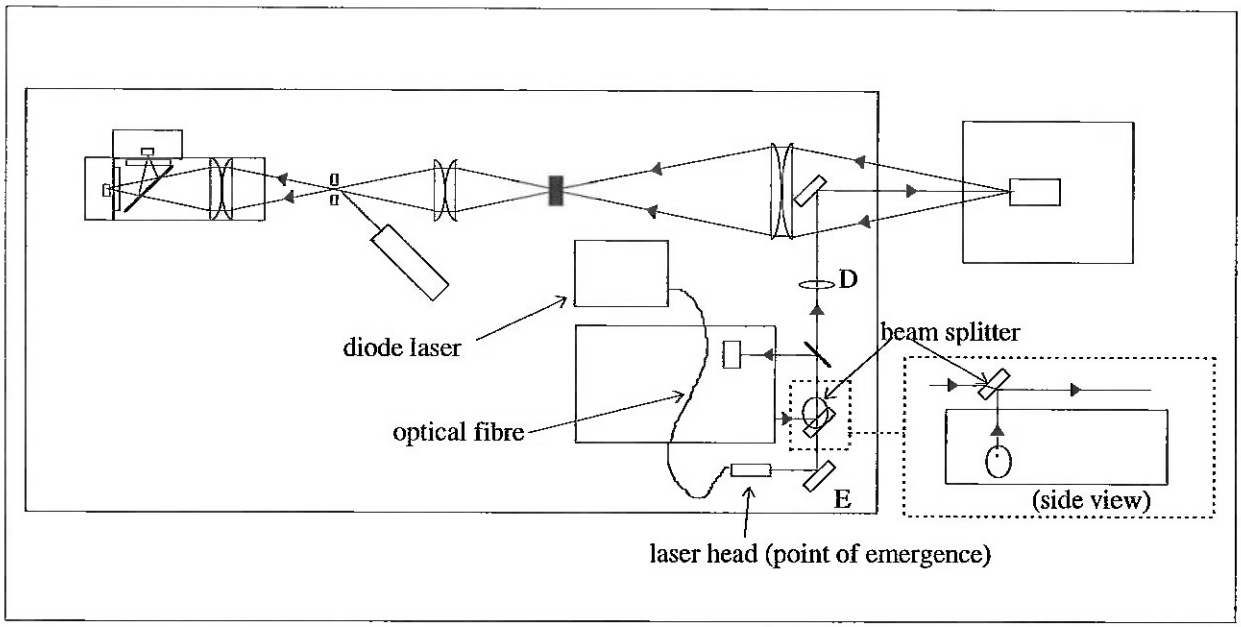

To assess the system's measurement of temperature, the laser induced signals were found as a function of furnace temperature as read by a thermocouple.

Results and Discussion

The YAG laser beam was found to have a (Gaussian) radius of ~1mm, three centimetres away from its point of emergence, as shown in figure 6. At the target, the beam was found not to have diverged appreciably. The limiting condition on the cross-sectional area of the beam is that it must not be greater than the active area of the detector. As the latter area was 30-40mm^2, the system had a considerable depth of field, although it was not necessary to make use of this freedom.

Figure 6. Investigating the YAG laser beam width

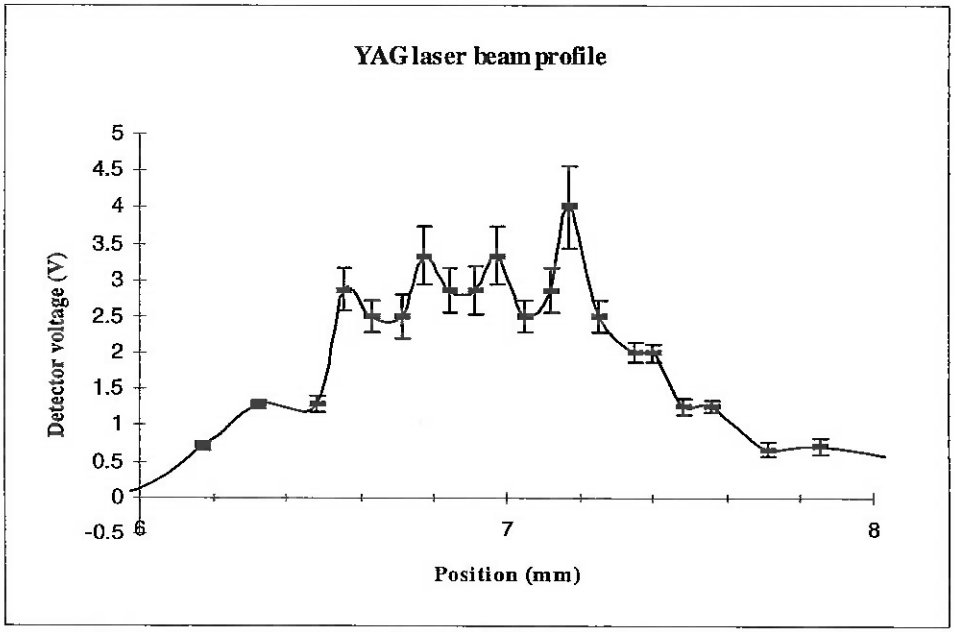

In channel one, with the (inconel) sample at 850°C, a laser induced signal of 3mV (RMS) was observed, but with a SNR (Signal to Noise Ratio) of only 6 ± 0.5. This was superposed with an approximately sinusoidal variation in signal of ~0.5mV (peak to peak) with a period of 4 ± 0.2 minutes that was due to the temperature of the furnace changing. With further investigation, it was found that the `noise' actually consisted of sharp decreases in signal followed by slow increases, on a time scale of 20-30 seconds. An example chart recorder trace is shown in Appendix C (image 1).

When the output of the Germanium laser power monitoring detector was observed on the same trace as the channel 1 signal, (Appendix C, image 2), a definite correlation was observed. As definite a correlation was found to exist between the signal and the power supply voltage (Appendix C, image 3). The 26Hz and 16Hz TTL reference signals coming from the two function generators were observed to be steady, which meant that the problem lay with the isolation chopper reference signal. It's amplitude was seen to be steady, but not it's frequency. The reason why a change in its frequency can produce a change in voltage is shown in figure 7, below.

Figure 7. Effect of unstable chopper frequency on average laser power

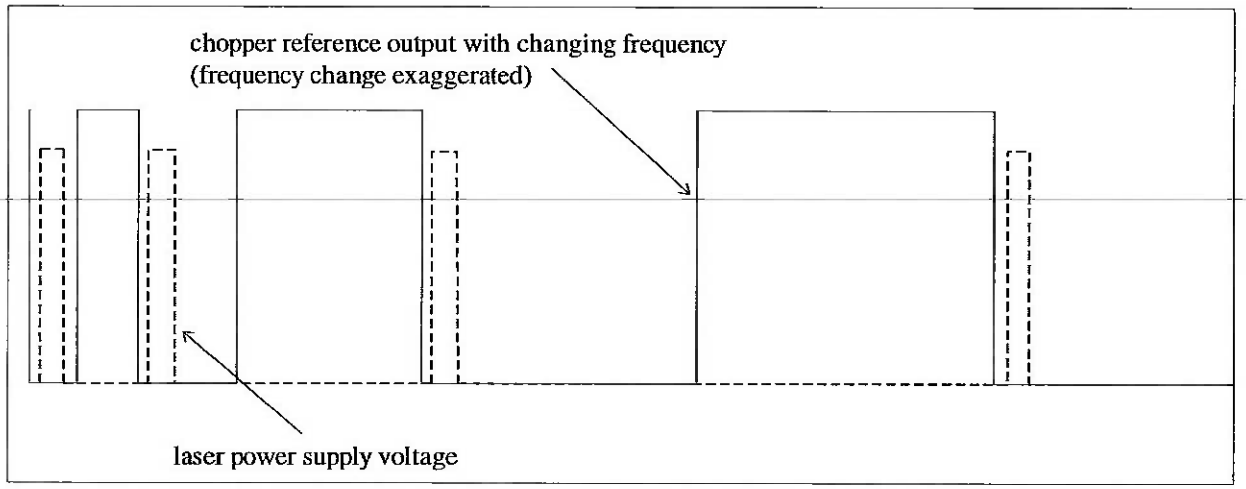

Over a given length of time, fewer pulses will appear within a 26Hz or 16Hz pulse, resulting in a decrease in net power. The frequency of the chopper was seen to vary in the same way as the signal, i.e. dropping suddenly then slowly increasing. This could suggest that the problem had a mechanical origin - a moving part being retarded in some way perhaps. The problem was solved by using a chopper that had a feedback mechanism controlling the voltage supply to the motor. With this new chopper, the laser power supply voltage was seen to be stable to greater than 1 part in 1000 (Appendix C, image 4).

An oscillation in laser power supply voltage was observed, which exhibited the characteristics of beating between the chopper and function generator signals. However, if the frequency of this oscillation is well outside the detection bandwidth of the system, then it will not make a significant contribution.

When the diameter of the iris aperture at point B (see figure 3) was increased from zero, the detected signal rose also, but then levelled off at 2.5 ± 0.2mm. This gives a measure of the extent to which the heat given to the sample by a (16Hz) laser pulse has been conducted away from the area covered by the laser beam. As the modulation frequency of the lasers is decreased, this critical diameter will increase as there will be more time for heat to flow in between pulses. The diameter was kept at this point and not increased further to minimise the detector current due to the passive sample radiation, which would give rise to excess shot noise in the detector.

With further work done to improve the optical alignment and the laser back scatter elimination scheme optimised, the signals obtained from inconel at 850°C were 19 ± 0.02mV in channel 1 giving a SNR of 1000 ± 50 and 3.2 ± 0.03 in channel 2 giving a SNR of 100 ± 10 (Appendix C, image 5). The noise voltages in each channel were approximately equal as expected, but the SNR in channel 1 was ~10 times larger than that in channel 2 because of the YAG laser's greater power and the properties of the sample.

If the system was working correctly, the ratio of the two signals should have been directly proportional to the derivatives of the corresponding Planck black body radiation functions. Figure 8 shows that this is indeed the case, within the uncertainty margins.

The line does not, however, go through the origin, as it should. Throughout this work, some DC offsets were present in channel 1 due to earth loops, but these problems were overcome as they arose and would change the shape of the graph instead of having the above effect. A plausible explanation involves the reliability of the thermocouple used to measure the temperature of the inconel sample. The values of temperature recorded are quite possibly inaccurate as the thermocouple used was not designed for use with the furnace, but was all that was available at the time.

Figure 8. LEFT system with inconel

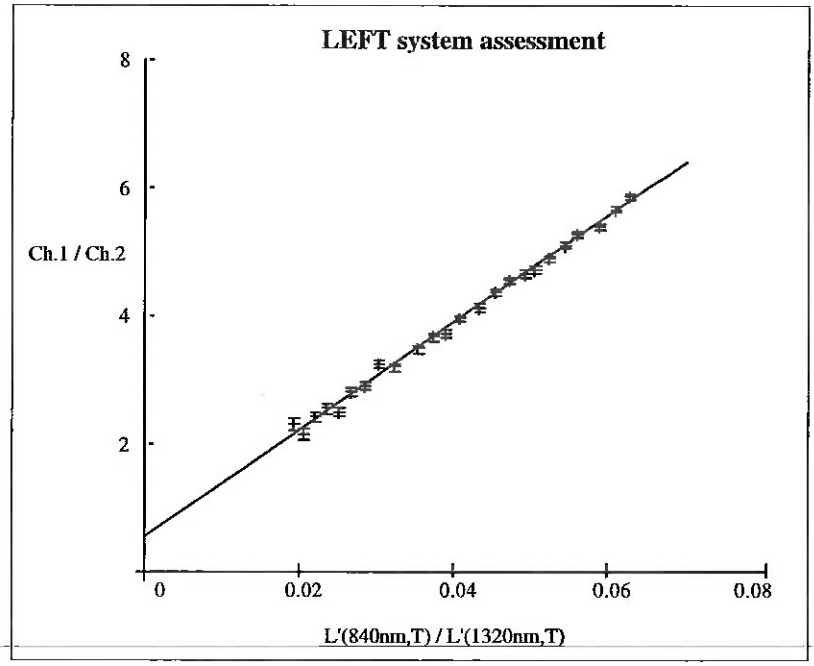

PART 2: THE LEVITATED DROP

2.1 INTRODUCTION

The levitated drop experiment in question was carried out in the Centre for Materials Measurement and Technology (C.M.M.T.) within the National Physical Laboratory. It consisted of a copper coil (made of pipe so that water could flow inside as a coolant) in which flowed an AC current of about 300 kHz (radio frequencies). Inside this coil was a tube of square cross-section made of optical quartz, in which a metal drop, ~5mm in diameter, was levitated. It was also heated as a result of currents induced by the coil's changing magnetic field. So that the oxidation of the surface of the drop could be controlled, a variable mixture of Hydrogen and Argon gases flowed inside the tube. The coil was wound such that there was a gap separating its upper and lower portions[3], so that emitted radiation could be focused onto the detectors.

This apparatus was used in the C.M.M.T. to measure the density and surface tension of the metal that formed the drop. The density was measured by photographing the drop using cameras with a calibrated length scale to find its volume and surface tension data was obtained by measuring the frequency at which `oblate-prolate' oscillations occurred within the drop when molten. The drop's temperature was measured using a standard two colour pyrometer.

2.2 ANALYSIS OF LASER INDUCED SIGNAL

Experimental Method

The LEFT system was set up with the levitated drop as the target. To do this, a screen was placed inside the coil with the tube removed and the image of the visible diode laser spot was focused onto this screen. To reconfirm that the alignment was sufficiently accurate, a hole was burnt into the (cardboard) screen by one laser to provide a target for the visible laser and then the process repeated for the other laser. One of the Silicon photodiode outputs

was connected to a digitising spectrum analyser, a Nickel drop was used and the YAG laser was used to characterise the noise on the signal obtained from the drop.

Results and Discussion

The laser power supply voltage was observed first, and was found to be highly noisy (SNR ~ 6), but this noise vanished when the RF field supporting the drop was turned off. The component responsible for this pick up was the power cable for the laser scatter elimination electronics. Rather than shield the cable, the ±15V power rails of the electronics in question were connected to ground through capacitors, filtering out this signal.

With a solid drop, laser induced signal (through channel 1) was observed, but with a SNR of 13 ± 0.5 (Appendix D, image 1). This was much lower than expected, and the results of Part 1 together with blocking the thermal radiation show that this noise was not due to the LEFT system itself. In the spectrum of the detected passive radiation signal, there was a peak at approximately 8Hz (Appendix D, image 2) varying between 3mV and 40mV (pkpk) on a time scale of tens of seconds. A direct correlation between this peak and the amplitude of vertical translational oscillations of the drop was found to exist (Appendix D, image 3). This was confirmed by tapping the unit to which the coil was attached. Through this tapping, other peaks were made to appear that were lower in frequency, thought to be due to drop oscillations in other directions. With a slightly larger drop, the same spectrum was observed, but with the aforementioned peak slightly lower in frequency.

When the drop had melted, the noise voltage had increased dramatically, approximately by a factor of a hundred. As the drop was melting the amplitude of its vibration increased to the extent that it frequently stuck to the side of the tube. The motion caused the noise to increase, but once molten, the drop was relatively stable and so this vibration can no longer be considered as a possible source of noise. In the spectrum of the noise voltage there were no obvious peaks. However, there was a marked increase in the general level of noise, and the noise increased with decreasing frequency (Appendix D, image 4).

To establish that the noise was caused by changes in drop radiance, the noise on the voltage due to the passive radiation in each channel was examined. There was found to be a correlation between the two and so the noise definitely was an attribute of the drop.

When checking with an infra-red viewer for laser back-scatter, a pattern in the reflected diode laser radiation was observed on the wall next to the apparatus. (The viewer responds to 840nm radiation much better than 1320nm radiation). When examined more closely, using a screen, this pattern was seen to have a random and mottled though stable nature. It was visible when the screen was held in front of the drop (without blocking the laser) and could be seen to move in phase with the vibrations of the drop. When the drop was made to vibrate in excess this motion increased to the extent that the pattern moved too fast to resolve any detail in the pattern. When the drop melted, the pattern vanished - in its place appeared homogenous radiation which swamped the laser scatter.

As the drop cools, it's temperature falls below its melting point and when solidification occurs latent heat is released in the form of a flash of radiation. For this reason, it is very clear when the drop has become solid. The pattern mentioned above was seen to re-appear immediately after this flash was seen and so coincided with the solidification of the drop.

The pyrometer that was measuring the drop's temperature gave a reading that did not alter significantly (by 0.3% at most). This was because the pyrometer uses the D.C. radiation emitted by the drop rather than the far smaller A.C. modulation that is measured by the LEFT system, and any noise signal at ~8Hz is greatly attenuated due to the pyrometer's integration time of approximately 0.5 seconds. These two facts mean that the pyrometer reading is expected to be stable.

Clearly there are two different regimes - one when the drop is solid and one when it is liquid.

With the solid drop, the pattern observed in the reflected laser radiation could have been due to spatial emissivity variations or surface structure on the drop. Both scenarios are possible as the drops were contaminated by some compound(s) on the surface, and they could be seen to be less smooth than a mirror. We know that the contaminants were there because they caused the drop to fizz and spit as it melted. The atmosphere inside the tube was controlled with the aim of minimising contamination, but it is not certain that this aim was completely

fulfilled. If there was some spatial emissivity variation then this, coupled with the vibration of the drop, could account for the observed changes in radiance. If, on the other hand, the observed pattern was due to three dimensional structure in the drop surface, then movement of the drop should have made no difference to the radiance. This is because the emission is hemispherical, i.e. independent of angle.

One other way in which drop vibration could have given rise to a large fluctuation in detected radiation is if the detector's field of view was not at all times covered by the drop. However, that was not the case as shown by the image of the drop that appeared on the iris aperture plate. The aperture was always covered by this image, and the noise increased gradually as drop vibration did, rather than a sudden increase that would be expected by the vibration becoming large enough for the above to occur.

When molten, the drop noise spectrum became more homogenous and increased in magnitude by approximately a factor of 100. To assess whether this effect could account for the observed noise, the noise spectrum ($N(\omega,t)$) was modelled as an exponential variation, and the gain of the system ($G(\omega)$) was assumed to have a Gaussian frequency dependence. The observed noise voltage at any time t is then:

$$V_{noise}(t) = \int_0^\infty G(\omega)\, N(\omega,t)\, d\omega$$

The calculation gave an instantaneous noise voltage that was highly comparable to that which was observed, showing that, whatever the source, the increase in noise occurred with little regard for frequency variation. The oblate-prolate drop oscillations mentioned in the introduction were not observed in the noise spectrum and are characteristically higher in frequency than the two modulation frequencies used so can be discounted as a possible noise source.

Considerable work has been done on the scattering of light due to surface waves at a planar fluid interface[4] (either liquid-liquid or liquid-vapour) for the purpose of making measurements of the same quantities that are measured using the levitated drop. In this field, a problem called "sloshing" was encountered, which is the passage of waves along the surface of a much lower frequency than those of interest. It was problematic because it greatly altered the direction in which the scattered light travelled. With a molten drop that is moving as a whole, the surface is definitely sloshing. As mentioned above, the emission should be independent of observation angle, and so sloshing would not seem to be a problem. If, however, there was a thin film present on the surface of the drop, then an angular dependence could be introduced due to interference, with the film exhibiting behaviour that could be related to that exhibited by a Fabry-Perot cavity. A thin film could be made of any coating which was on the drop before melting, or appeared after the melt, which had since become molten itself, and so coated the drop. This idea is commensurate with the observed frequency spectrum of the noise voltage, as one would expect that voltage fluctuations due to this phenomenon would decrease at high frequencies.

In addition to a high level of noise, there is a factor which decreases the observed signal strength, and this is the sample emissivity, which was estimated to be as low as 0.1 on some samples. Compared with the previously used Inconel sample, the signals would be smaller by a factor of $0.1^2/0.8^2 = 0.015$ as they depend upon the square of the sample's emissivity.

All of the above was observed through channel 1. The laser induced signal obtained with a solid drop in channel 2 was approaching the limit of detectability with a SNR of approximately 4 (Appendix D, image 5).

3 CONCLUSION

A portable prototype LEFT system was constructed and was shown to perform successfully with a suitable sample. However, the levitated drop proved to be a difficult target for LEFT. This is because the lasers used in LEFT induce very small signals which are a challenge to detect under controlled circumstances and even more so when there is an excess of noise and low emissivity, as there was with the levitated drop.

Temperature measurement on the solid drop was possible, although with a very large standard deviation. When the drop had melted, the noise was so great that the signals were swamped and temperature measurement was no

longer possible with LEFT. The pyrometer could still function because it used the large DC thermal radiation signal instead of the very small AC modulated signal.

The above work shows that the LEFT system in its current form is more suited to stationary samples than those like the levitated drop and that more work will have to be done on the technique before it can replace pyrometers in such harsh conditions.

The following suggestions could be included in any further work done in this area:

- A (chemically) cleaned golden drop would have had a much reduced surface coating as it would react very little with its environment. By looking at the signals obtained from this drop it could be definitely established whether surface coatings were responsible for apparent emissivity fluctuations.

- Painting the drop black with a high temperature paint such as pyromet would raise the emissivity to approximately one and so increase the observed laser induced signals by a factor of up to 100.

- Isolating the whole drop apparatus is an option that would reduce or remove drop vibration so that LEFT could be applied. This need not be as expensive as it first appears, because a crude but effective support could be made from any compressible material, for example car tire inner-tubes. The weight of the apparatus combined with a sensible tube pressure could produce a resonant frequency low enough to eliminate the effects of external vibration.

- The modulation (and therefore detection) frequencies could be moved to the region between 50Hz and 100Hz. The noise spectrum showed that in this frequency range there was little noise and it would be away from mains frequency and first overtone. The amplitude of laser induced signal is inversely proportional to the square root of the modulation frequency and so would decrease, however the SNR would be likely to increase.

- The laser induced signal is directly proportional to laser power, and so an increase in laser power would improve the SNR still further.

- A P.C. based data acquisition program using an analogue to digital converter card will eventually take the place of the two Lock-in Amplifiers and so it would be useful to assess the effect of the noise on this system.

APPENDIX A

Assessment of photodiode performance.

All voltages were observed with no radiation falling onto the detectors using a Lock-in amplifier with a 12dB per octave gain decay and 1 second time constant. Therefore, the bandwidth is 0.25Hz throughout.

Silicon photodiode with external pre-amplifier:

Responsivity, R, = 0.45 A/W
Noise Equivalent Power, NEP, = 0.055 $pWHz^{-1/2}$
Feedback resistance, R_{fb}, = 47 MΩ

System gain = 40 dB

∴ Expected RMS noise voltage $= R.NEP.\sqrt{B} \times 100 \times R_{fb}$

$= 58.2\mu V$

Observed RMS noise voltage $= 1.07\ mV$

This value is larger than expected by a factor of ~18, but was found to be due to the pre-amplifier and not the detector itself.

Hamamatsu Silicon photodiode:

R = 0.5 A/W
NEP = 0.1 $pWHz^{-1/2}$
R_{fb} = 1.8MΩ

∴ Expected RMS noise voltage $= R.NEP.\sqrt{B} \times 100 \times R_{fb}$

$= 4.5\ \mu V$

Observed RMS noise voltage $= 25\ \mu V$

This value is ~5 times larger than expected.

Germanium photodiode:

R = 0.95 A/W
NEP = 0.6 $pWHz^{-1/2}$
R_{fb} = 820 kΩ

∴ Expected RMS noise voltage $= R.NEP.\sqrt{B} \times 100 \times R_{fb}$

$= 23.4\ \mu V$

Observed RMS noise voltage $= 21.5\ \mu V$

The quoted values for responsivity and noise equivalent power are for when the electronic cooler is in operation. As it was not when the above data was taken, it is likely that the observed noise voltage is far less than expected. The most probable explanation is that the bandwidth value of 0.25Hz is an unreliable estimate. A more accurate value could be obtained using two function generators; one as a reference signal and the other as an input of known frequency.

APPENDIX B

Experiment Layout.

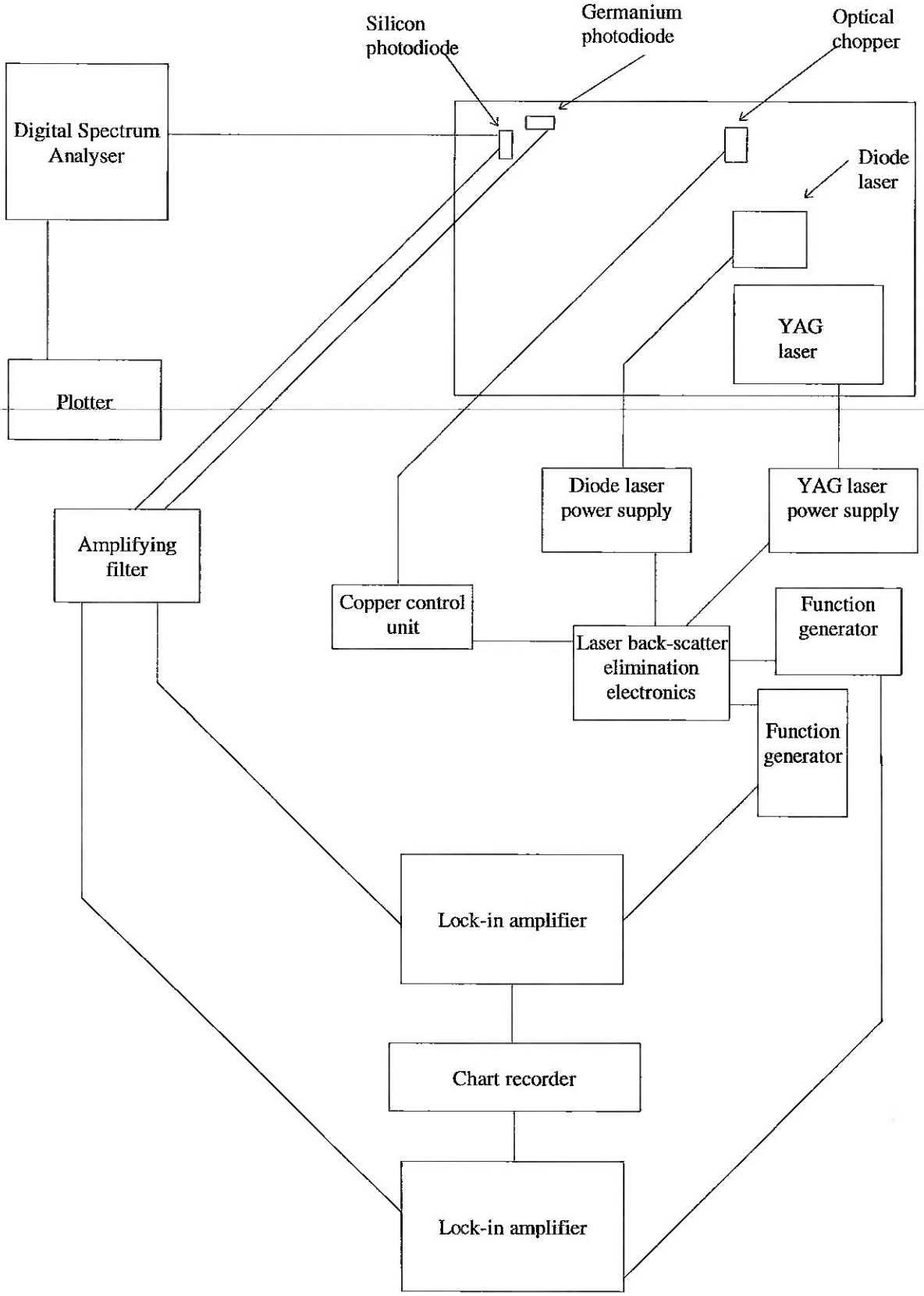

APPENDIX C

Thermal Modulation results.

1. Laser induced signal in channel 1 from furnace at 850°C.

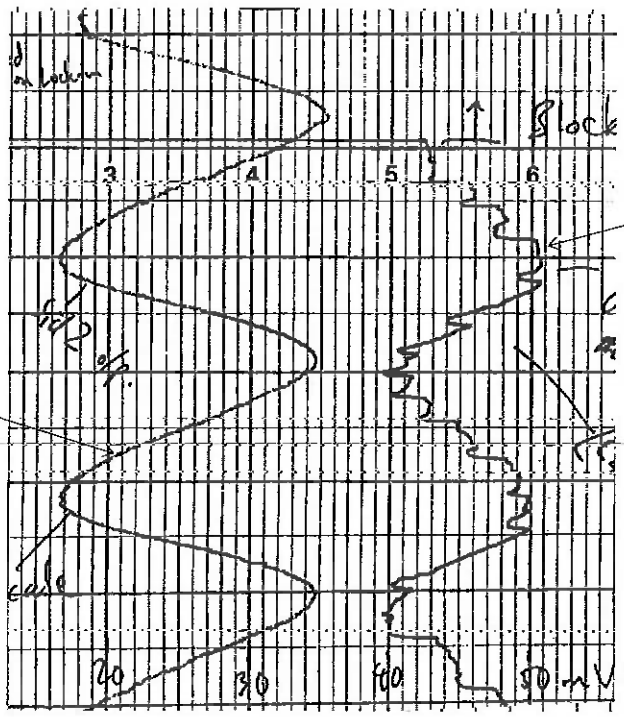

2. Trace showing correlation between laser power and channel 1 signal.

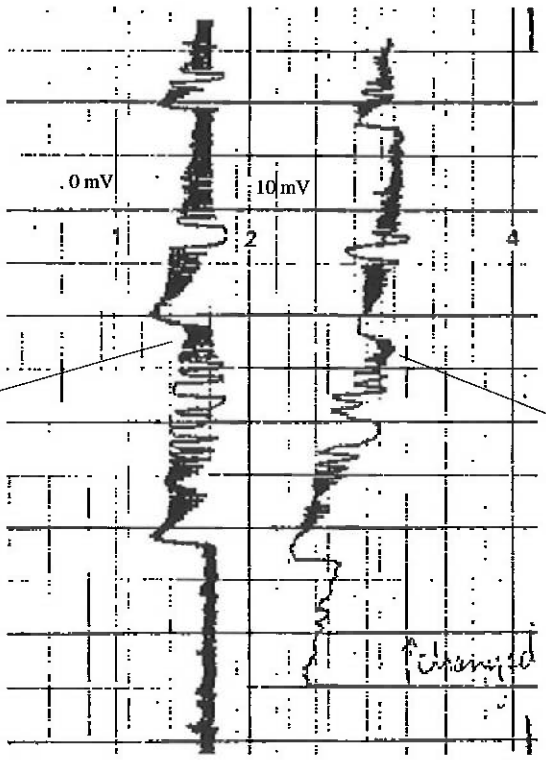

3. Trace showing correlation between channel 1 signal and laser power supply voltage.

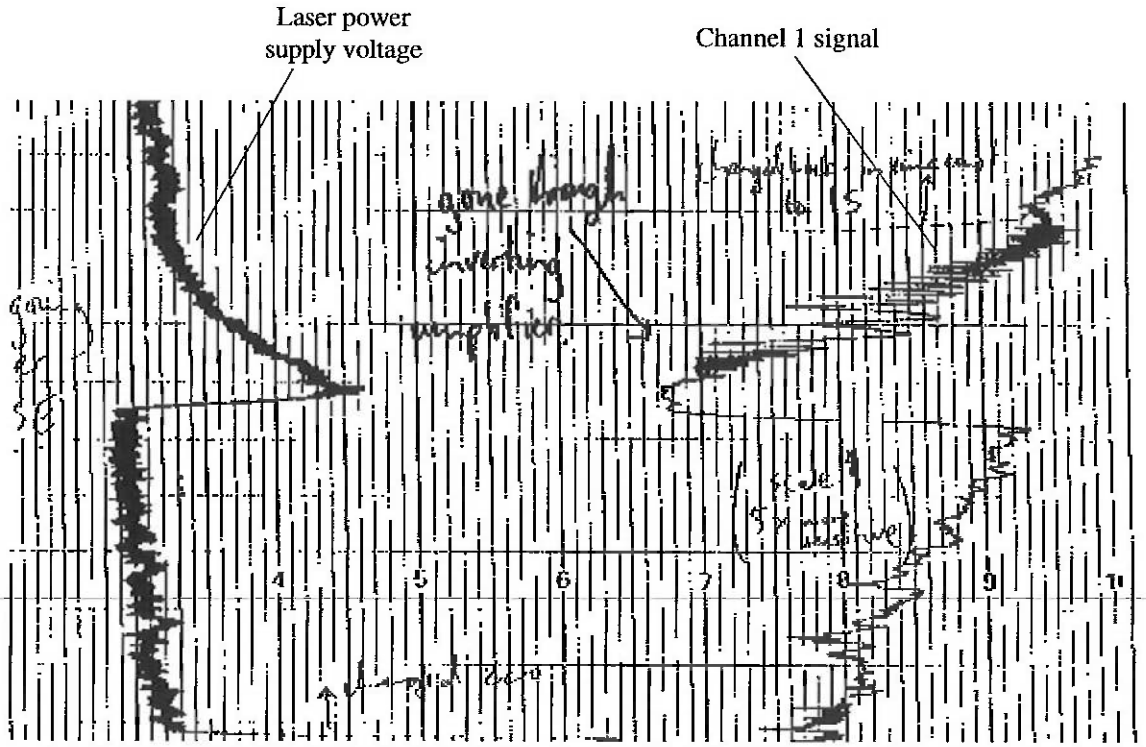

(Chart speed = 10cm/min)

4. Trace comparing chopper frequency stability and illustrating RF pick-up.

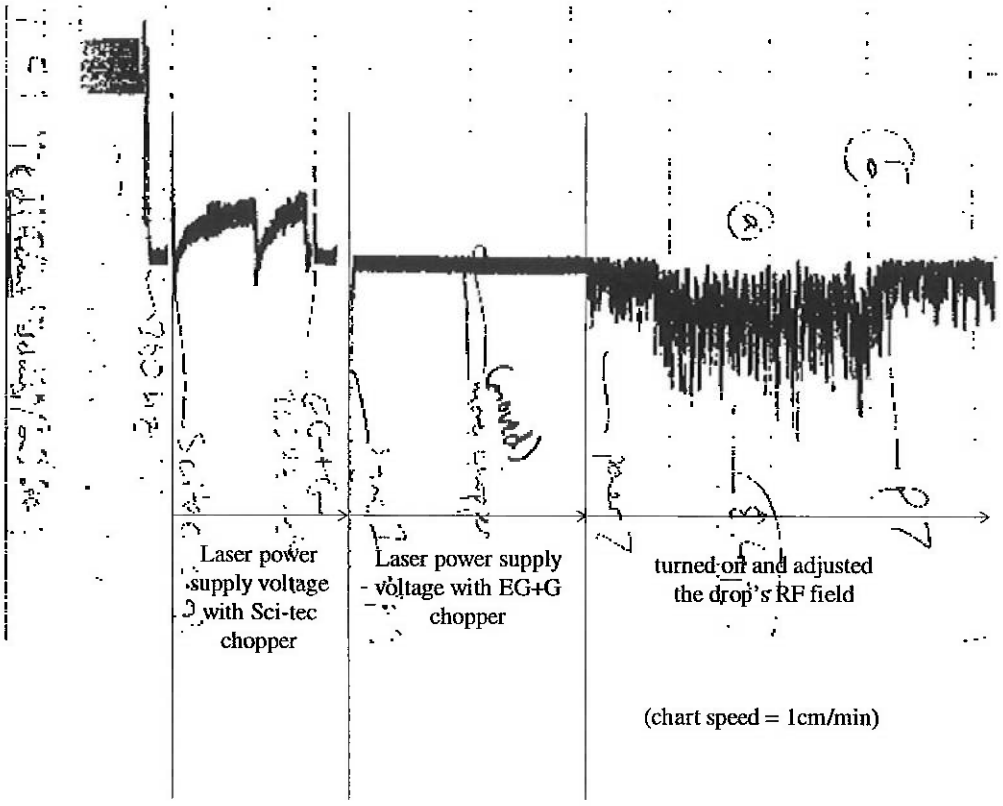

(chart speed = 1cm/min)

5. Trace showing signals in both channels.

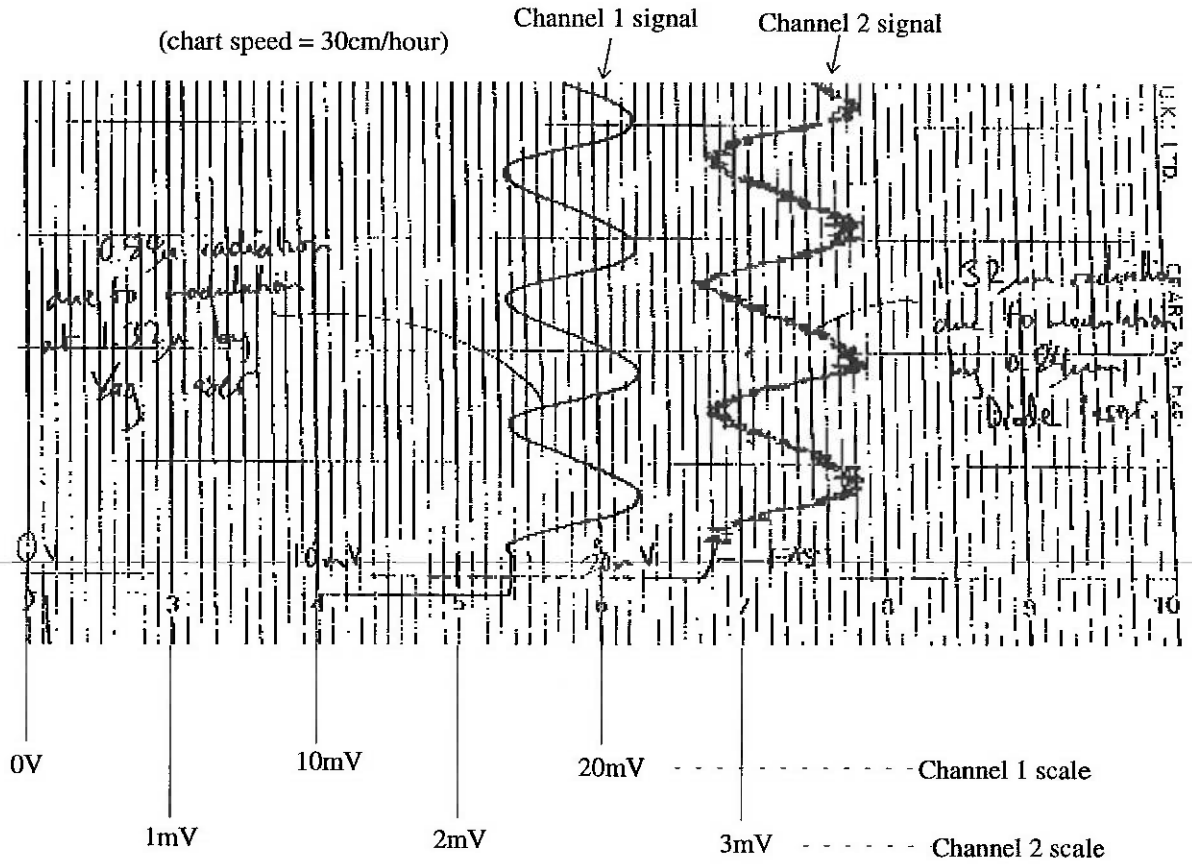

APPENDIX D

Levitated drop signal analysis.

1. Trace showing Channel 1 signal obtained from the levitated drop, when solid.

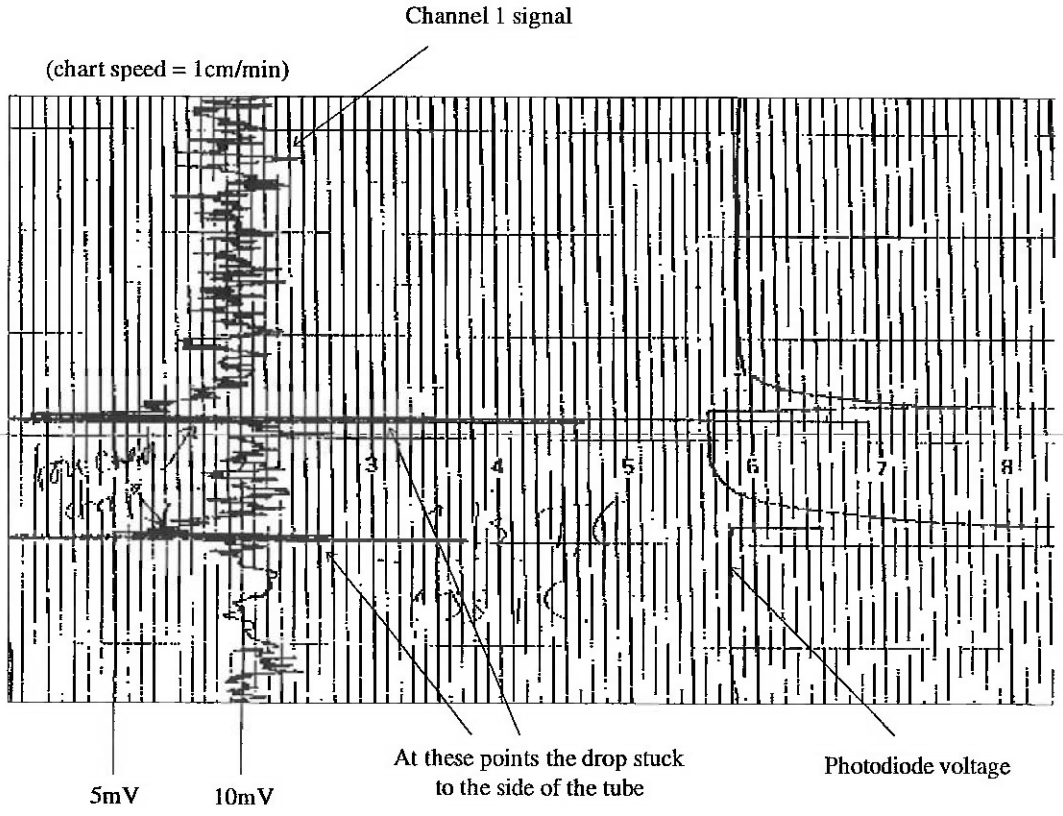

2. A typical frequency spectrum of the current induced by the radiation emitted by the solid drop.

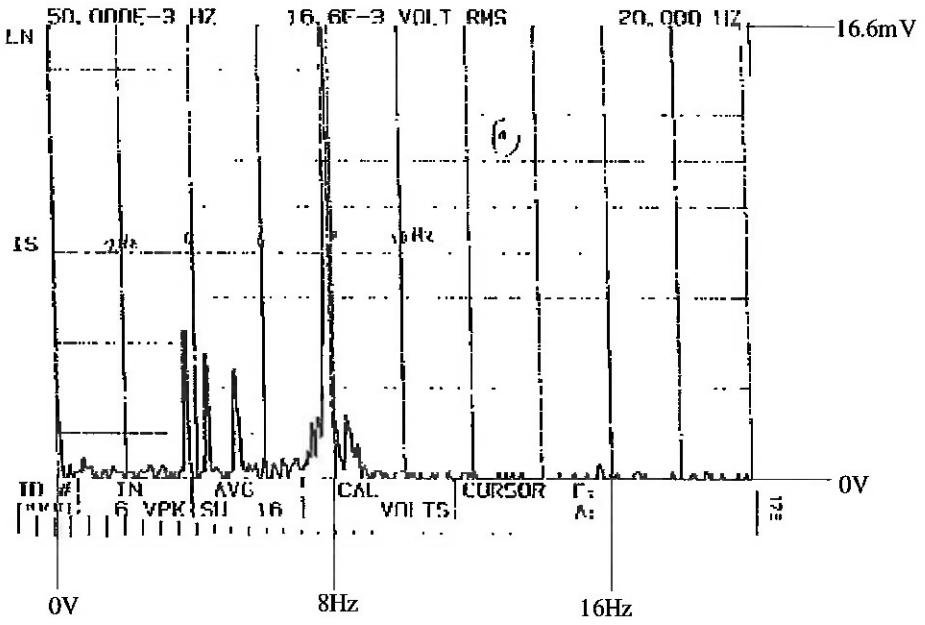

3. Trace showing a correlation between signal noise and drop vibration.

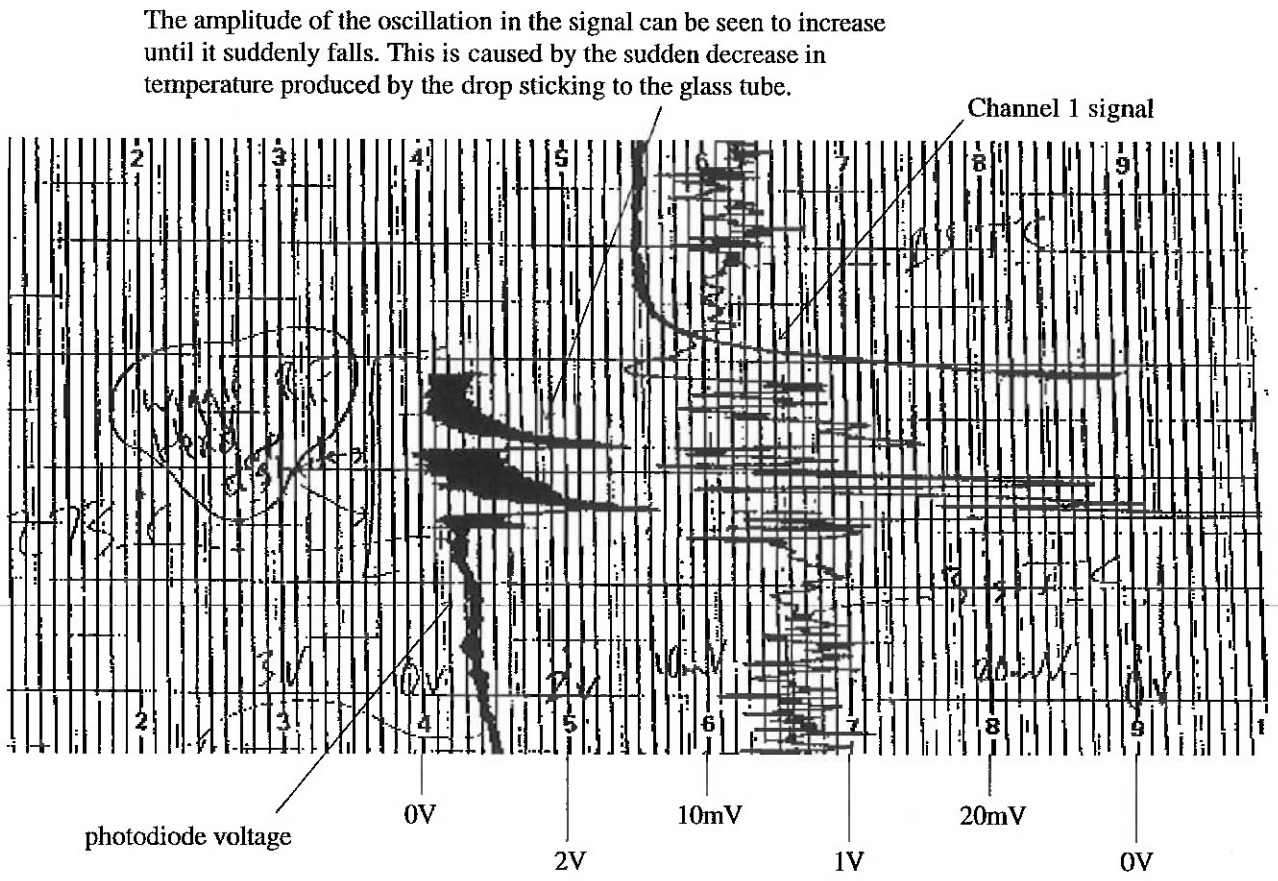

4. A typical frequency spectrum of the current induced by the radiation emitted by the liquid drop.

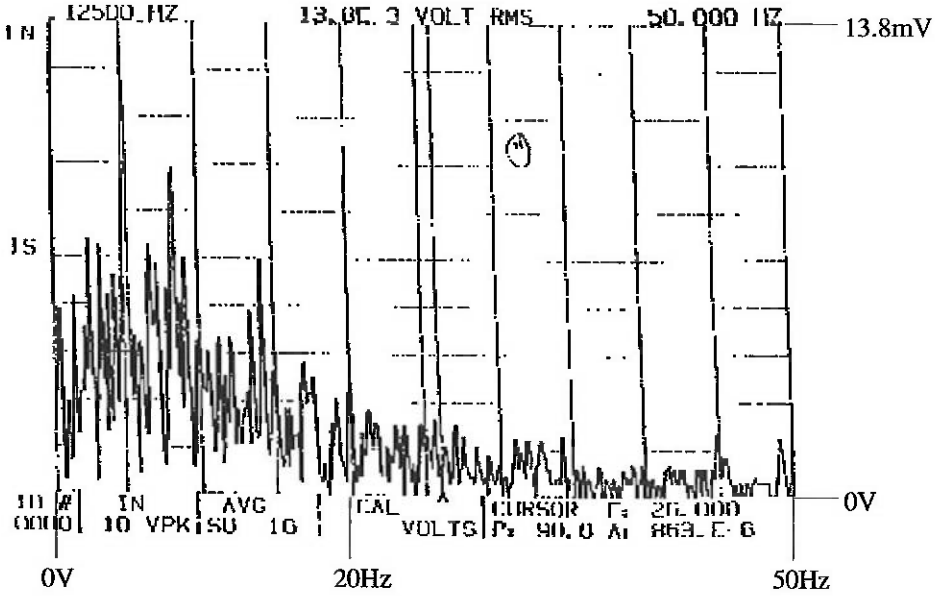

5. Channel 2 signal.

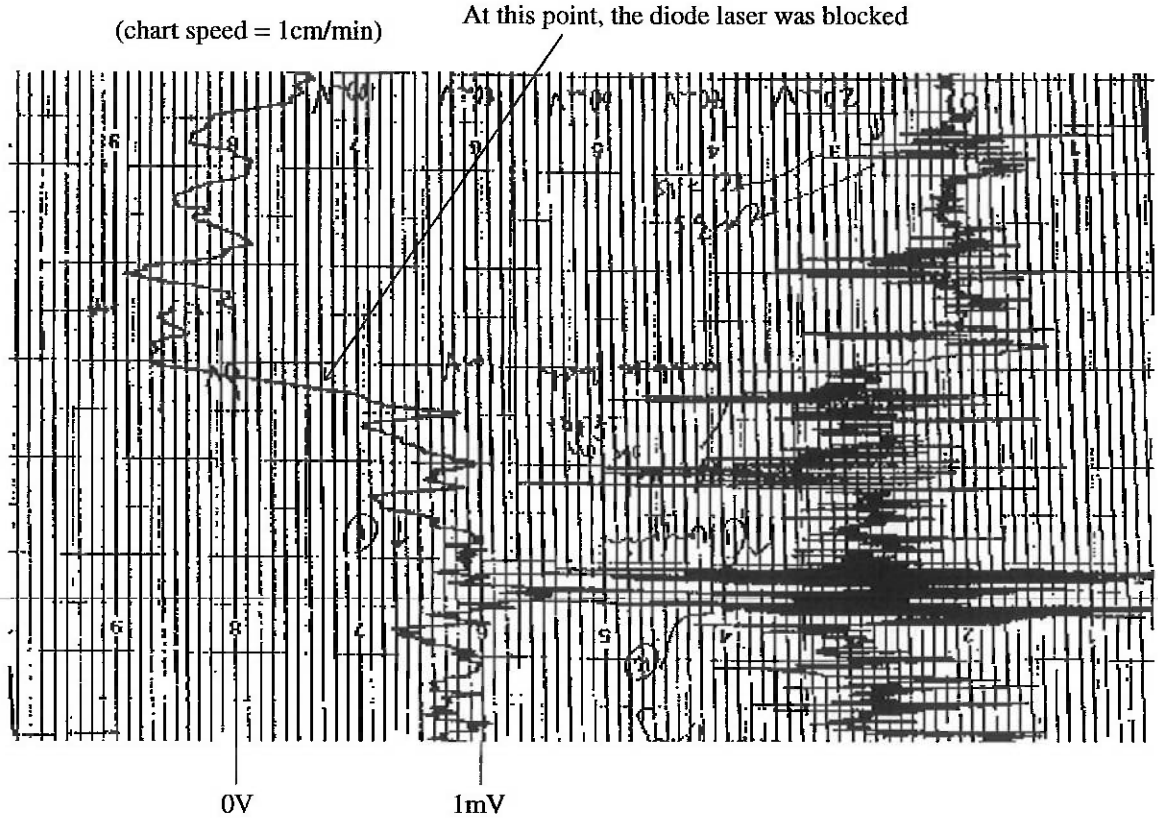

APPENDIX E

Photo Gallery

1. The LEFT apparatus.

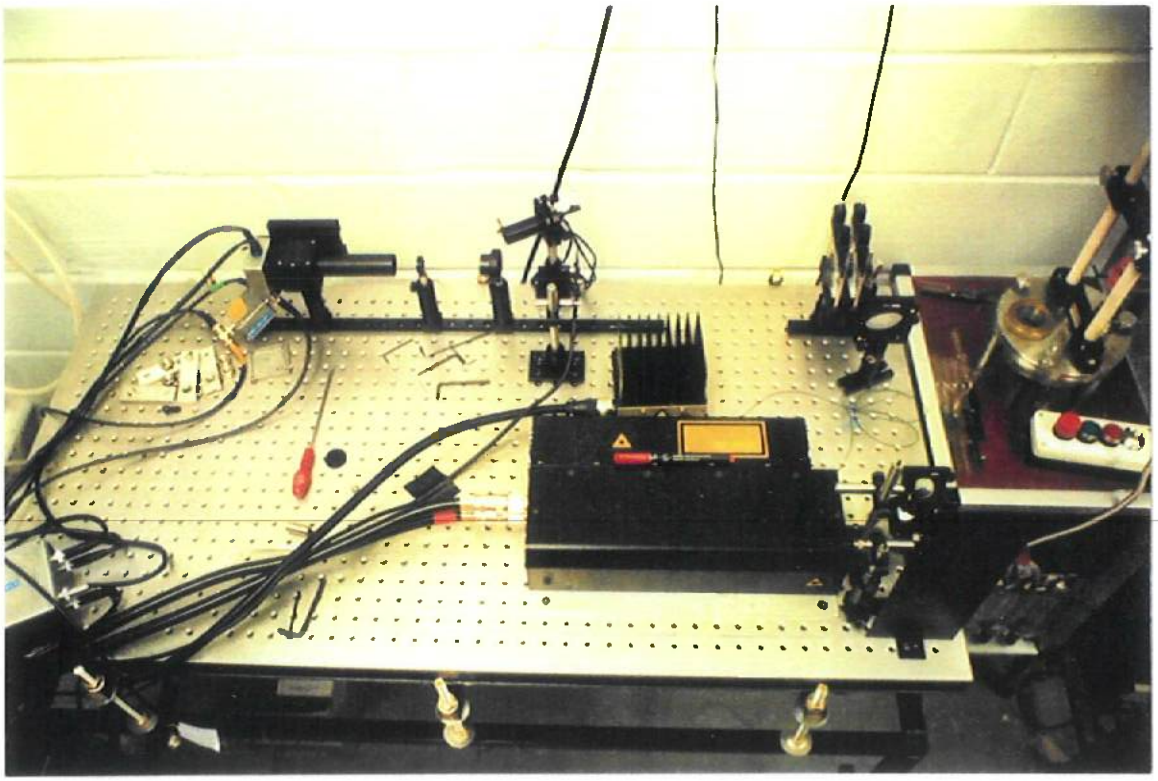

2. The levitated drop apparatus.

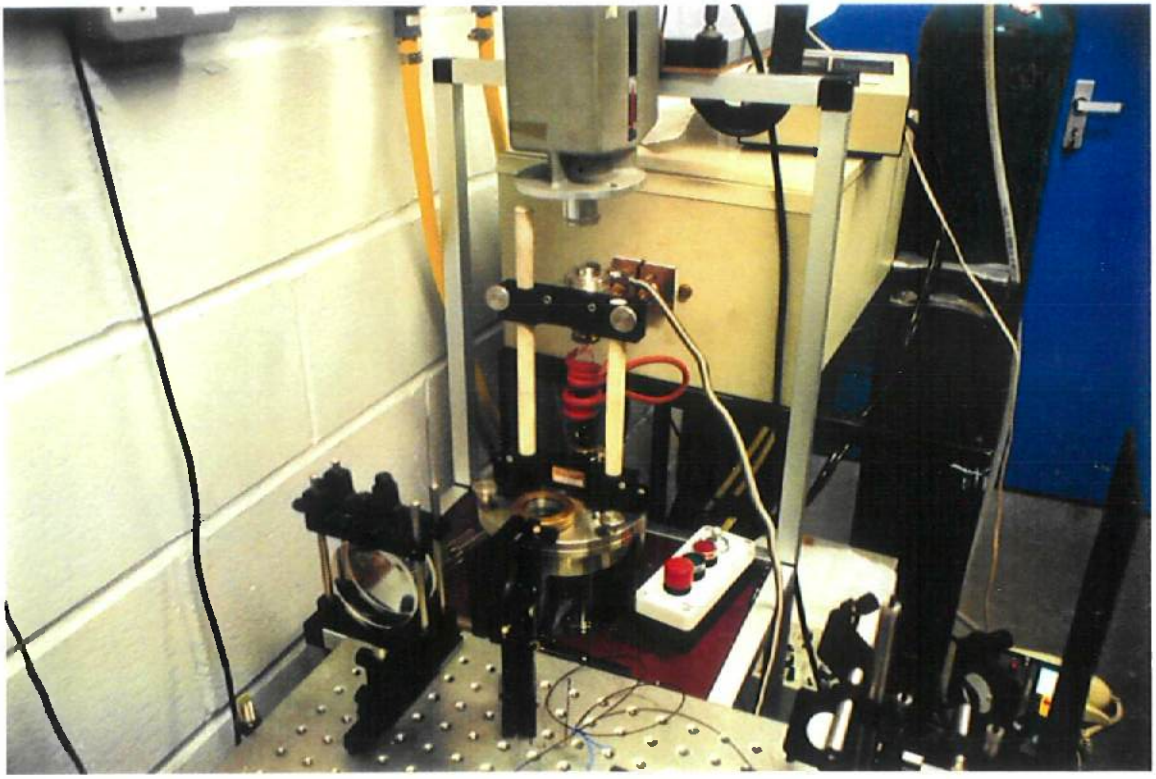

3. The LEFT system showing controlling electronics.

REFERENCES

1 Throughout the introduction, the reader is referred to the work of Dr. G. J. Edwards, Centre for Quantum Metrology, National Physical Laboratory. Due to the early stage of development of LART techniques, there is a shortage of published material regarding them, hence the non-specificity of reference 1.

2 For all information regarding experimental method and logistics the reader is referred to the author's laboratory note book.

3 The work of Robert Brooks, Centre for Materials Measurement and Technology, National Physical Laboratory.

4 W.V. Meyer*, P. Tin, J. A. Mann, Jr, H. M. Cheung, R.B. Rogers, L. Lading.
A preview of a modular surface light scattering instrument with autotracking optics.

* NASA Lewis / OAI,
M.S. 105-1
21000 Brookpark Road,
Cleveland,
OH 44135-3191 USA